

# The $R$ - $S$ model for magnetic systems with competing interactions: series expansions and some rigorous results†

S Redner‡§|| and H E Stanley‡§

‡Department of Physics, Massachusetts Institute of Technology, Cambridge, Massachusetts 02139, USA

§Department of Physics, Boston University, Boston, Massachusetts 02215, USA

Received 26 May 1977

**Abstract.** We study the properties of a model system that exhibits a transition between ferromagnetic and helical order at a Lifshitz point, as interaction parameters  $R$  and  $S$  compete. Here  $R \equiv J_z/J_{xy}$  and  $S \equiv J_z'/J_{xy}$ , where  $J_z$  and  $J_z'$  denote interactions between nearest-neighbour and next-nearest-neighbour spin pairs respectively in the  $z$  direction, and  $J_{xy}$  is a nearest-neighbour interaction between spin pairs in each  $xy$  plane. We calculate the high-temperature susceptibility series to order 8, 6, 5, and 35 respectively for the Ising, planar, Heisenberg, and spherical models ( $n = 1, 2, 3$ , and  $\infty$ ). In order to verify our results, we derive rigorous results which provide strong checks on the series coefficients. Series analysis is focused on the ferromagnetic phase. In particular, we confirm scaling with respect to both parameters  $R$  and  $S$ . In addition, we find the critical region shrinks as the Lifshitz point is approached. This is indicated by analysing the spherical model series where asymptotic series behaviour is not evident, even at order 35. Finally, by exploiting simple geometric ideas about the dependence of the correlation length on  $R$  and  $S$ , we describe the full wavevector and temperature dependence of the structure factor.

## 1. Introduction

Recently, much attention has been given to the following  $n$ -vector Hamiltonian

$$\begin{aligned} \mathcal{H} &= -J_{xy} \sum_{i,j} \mathbf{s}_i \cdot \mathbf{s}_j - J_z \sum_{i,j} \mathbf{s}_i \cdot \mathbf{s}_j - J_z' \sum_{i,j} \mathbf{s}_i \cdot \mathbf{s}_j \\ &\equiv -J_{xy} \left( \sum_{i,j} \mathbf{s}_i \cdot \mathbf{s}_j + R \sum_{i,j} \mathbf{s}_i \cdot \mathbf{s}_j + S \sum_{i,j} \mathbf{s}_i \cdot \mathbf{s}_j \right), \end{aligned} \quad (1)$$

where the first two sums are over nearest-neighbour pairs in the same and adjacent  $xy$  planes respectively, and the third sum is over next-nearest-neighbour spin pairs along the  $z$  axis only (cf figure 1(a)). This Hamiltonian was first introduced by Elliott (1961), and the recent interest in this model is due to the fact that it exhibits a transition, as  $R$  and  $S$  vary, between ferromagnetic and helical order at a Lifshitz point (Hornreich *et al* 1975a, b; Nicoll *et al* 1976a, b). The helical phase arises from the competition between the interactions  $R$  and  $S$ . When  $S/|R|$  is sufficiently negative, the helical phase is energetically favoured.

† This work was supported in part by the NSF and the AFOSR.

|| Present address: Physics department, University of Toronto, Toronto, Canada.

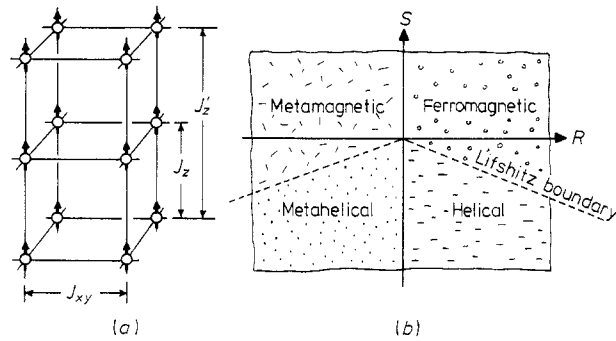


**Figure 1.** (a) The three interactions included in the Hamiltonian (1). (b) The  $R$ - $S$  model phase diagram for  $T = 0$ , showing the four ordered phases and the Lifshitz boundary.

In this paper we will study the ferromagnetic phase of this system by using high temperature series, while the properties near the Lifshitz point, and in the helical phase will be treated elsewhere (Redner and Stanley 1977). Using both mean-field theory (cf Appendix 1) and exact results for the case  $n = \infty$  (cf Appendix 2), it is predicted that helical order exists for  $S < -|R|/4$ , and that spatially uniform order exists for  $S > -|R|/4$ . Here, spatially uniform order means ferromagnetism for  $R > 0$ , and metamagnetism for  $R < 0$ . Because of the symmetry of the system, corresponding 'staggered'† thermodynamic functions for  $R < 0$ , and 'direct' thermodynamic functions for  $R > 0$  are identical. Therefore in what follows, we consider the case  $R > 0$  only. Since the two parameters  $R$  and  $S$  determine the type of order that exists, we call the model Hamiltonian (1) the  $R$ - $S$  model. Figure 1(b) is a schematic phase diagram.

An interesting feature of the ferromagnetic phase is that series analysis indicates exponents which appear to vary continuously with  $R$  and  $S$ , and this variation is quite large near the Lifshitz boundary. However, according to the renormalisation group, one set of universal exponents exists in the ferromagnetic phase, while a different set of exponents exists in the helical phase (Droz and Coutinho-Filho 1976, Garel 1976, Garel and Pfeuty 1976). Consequently, the exponents will change discontinuously as  $R$  and  $S$  vary through the Lifshitz point.

These apparently conflicting results are reminiscent of the situation found in anisotropic systems. This type of system may be described by the  $R$ - $S$  model with  $S$  set equal to 0. It is well known that for any  $R \neq 0$  the exponents are those of a three-dimensional system, while for  $R = 0$  the exponents change discontinuously to two-dimensional values. Analysis of finite length series indicates exponents that vary continuously from three- to two-dimensional values as  $R \rightarrow 0$ , and the interpretation of this was the source of some controversy. Oitmaa and Enting (1971, 1972) claimed that the analysis results conflicted with universality, while Rapaport (1971) pointed out that a continuous variation must occur if only a finite number of series terms are analysed, and as  $R \rightarrow 0$  progressively more terms are required to probe asymptotic behaviour.

The same conclusion was reached independently by Paul and Stanley (1971, 1972), who found that for small  $R$  the first few exponent estimates based on successive ratios of series terms appeared to extrapolate to the two-dimensional value, while at high order a trend to the three-dimensional value was evident. Moreover, they computed and analysed

† By staggered, we mean alternation in successive  $xy$  planes, rather than site alternation.

series of order 20 for the spherical model ( $n = \infty$ ), and found that as  $R$  decreased, the order at which the true asymptotic behaviour was evident, increased. Thus the use of the spherical model series served as an important tool in understanding the asymptotic behaviour of the Ising series as  $R$  becomes small, and as the critical region becomes correspondingly small. Because the exponent behaviour near the Lifshitz point is not unlike that found in anisotropic systems, the  $n = \infty$  series will therefore be used as a tool for understanding asymptotic series behaviour.

In § 2 we outline the series calculation procedure. We also derive rigorous results for the  $R$ - $S$  model susceptibility, and apply these to check certain of the series coefficients. In § 3, we analyse the series in the ferromagnetic phase and confirm scaling with respect to both parameters  $R$  and  $S$ . In § 4, we study the susceptibility series for both  $n = 1$  (Ising) and  $n = \infty$ , and we give a simple geometric interpretation of the fact that asymptotic behaviour near the Lifshitz point sets in only at very high order. Then, in § 5, we discuss how this interpretation provides an understanding of the full wavevector and temperature dependence of the structure factor.

## 2. The series and a rigorous result

Using the renormalised linked-cluster theory (Wortis *et al* 1969, Wortis, 1974), we have calculated the coefficients  $a_l(R, S)$  in the zero-field susceptibility series

$$\chi = \sum_{l=0}^L a_l(R, S)(\beta J_{xy})^l \quad (2)$$

for Ising, planar, and Heisenberg spins ( $n = 1, 2, 3$ ) to order  $L = 8, 6$ , and 5 respectively. Here  $\beta = 1/kT$ . We calculate the  $a_l(R, S)$  for  $(L + 1)(L + 2)/2$  different combinations of  $J_{xy}$ ,  $R$ , and  $S$ , and use these results to solve simultaneous linear equations to determine the coefficients  $A_{jkl}$  in the multinomial†

$$a_l(R, S) = \sum_{j+k \leq l} A_{jkl} R^j S^k \quad (3)$$

For  $n = 1$ , the three-variable series in  $\beta J_{xy}$ ,  $R$ , and  $S$  is also re-expressed in the form

$$\chi = \sum_{l=0}^L \sum_{j+k \leq l} B_{jkl} \tanh^{l-j-k}(\beta J_{xy}) \tanh^j(\beta J_z) \tanh^k(\beta J'_z) \quad (4)$$

In (4), the coefficients  $B_{jkl}$  are all integers. The coefficients  $B_{jkl}$  for  $n = 1$ , and  $A_{jkl}$  for  $n = 2$  and 3 are presented in tables 1–3. Hence from (3) and (4), the  $a_l$  may be computed directly. This results in an enormous saving of computer time when series for many different values of  $R$  and  $S$  are required.

Moreover, by expressing our results for arbitrary  $J_{xy}$ ,  $R$ , and  $S$  we can check many of the  $A_{jkl}$  and  $B_{jkl}$ . Firstly, we verify known results for the linear chain, the square lattice, and the simple cubic lattice by taking the respective limits  $J_z = \infty$ ,  $J'_z = 0$ ;  $J_z = 0$ ,  $J'_z = \infty$ ;  $J_z = J'_z = 0$ ;  $J_z = J_{xy}$ ,  $J'_z = 0$ ; and  $J_z = 0$ ,  $J'_z = J_{xy}$ . More thorough checks are provided by generalising to  $S \neq 0$ , the  $S = 0$  theorems of Liu and Stanley (1972, 1973) (see

† For example, when  $n = 1$ :  $a_0 = 1$ ,  $a_1 = 4 + 2R + 2S$ ,  $a_2 = 12 + 16R + 2R^2 + 8RS + 16S + 2S^2$ ,  $a_3 = 34\frac{2}{3} + 80R + 32R^2 + 1\frac{1}{3}R^3 + 96RS + 10R^2S + 16RS^2 + 80S + 32S^2 + 1\frac{1}{3}S^3$ .

**Table 1.** The coefficients  $B_{jkl}$  in the reduced susceptibility series for  $n = 1$ , simple cubic lattice.

$$\chi \simeq \sum_{l=0}^8 \sum_{j+k \leq l} B_{jkl} \tanh^{l-j-k}(\beta J_{xy}) \tanh^j(\beta J_z) \tanh^k(\beta J_z).$$

(a)  $k = 0$  (all entries check with Harbus and Stanley 1973b).

$l \backslash j$	0	1	2	3	4	5	6	7	8
0	1								
1	4	2							
2	12	16	2						
3	36	80	32	2					
4	100	336	240	48	2				
5	276	1264	1392	512	64	2			
6	740	4432	6680	3888	888	80	2		
7	1972	14768	29136	23600	8544	1376	96	2	
8	5172	47376	116528	124720	63216	16080	1968	112	2

(b)  $k = 1$

$l \backslash j$	0	1	2	3	4	5	6	7
1	2							
2	16	8						
3	80	96	10					
4	336	672	240	8				
5	1264	3680	2360	384	8			
6	4432	17376	17168	5504	512	8		
7	14768	74208	100000	52032	10032	640	8	
8	47376	294624	517648	378272	120960	15872	768	8

(c)  $k = 2$

$l \backslash j$	0	1	2	3	4	5	6
2	2						
3	32	16					
4	240	288	28				
5	1392	2720	928	16			
6	6680	19040	11664	1632	10		
7	29136	110336	104192	10400	2112	16	
8	116528	563680	725488	350304	58400	2560	16

Table 1.—continued

(d)  $k = 3$

$l \backslash j$	0	1	2	3	4	5
3	2					
4	48	24				
5	512	608	58			
6	3888	7520	2512	24		
7	23 600	65 760	39 336	4992	-20	
8	124 720	461 344	424 432	116 352	6144	24

(e)  $k = 4$

$l \backslash j$	0	1	2	3	4
4	2				
5	64	32			
6	888	1056	100		
7	8544	16 448	5440	32	
8	63 216	175 520	103 616	12 384	-132

(f)  $k = 5$

$l \backslash j$	0	1	2	3
5	2			
6	80	40		
7	1376	1632	154	
8	16 080	30 880	10 160	40

(g)  $k = 6$

$l \backslash j$	0	1	2
6	2		
7	96	48	
8	1968	2336	220

(h)  $k = 7$

$l \backslash j$	0	1
7	2	
8	112	56

Table 1.—continued

(i)  $k = 8$

	$j$	0
$l$		
8		2

Table 2. The coefficients  $A_{jk}$  in the reduced susceptibility series for  $n = 2$ , simple cubic lattice.

$$\chi \simeq \sum_{l=0}^6 \sum_{j+k \leq l} A_{jk} (\beta J_{xy})^l R^{-j} S^k.$$

(a)  $k = 0$  (all entries check with Lambeth and Stanley 1975).

	$j$	0	1	2	3	4	5	6
$l$								
0		1						
1		4	2					
2		12	16	2				
3		34	80	32	1			
4		88	328	240	40	0		
5		$219\frac{1}{3}$	1184	1372	468	32	$-\frac{1}{3}$	
6		529	$3917\frac{1}{3}$	6416	3656	640	$13\frac{1}{3}$	$-\frac{1}{6}$

(b)  $k = 1$

	$j$	0	1	2	3	4	5
$l$							
1		2					
2		16	8				
3		80	96	10			
4		328	672	240	2		
5		1184	3632	2360	320	$-5\frac{1}{2}$	
6		$3917\frac{1}{3}$	16704	17008	5032	212	$-2\frac{2}{3}$

(c)  $k = 2$

	$j$	0	1	2	3	4
$l$						
2		2				
3		32	16			
4		240	288	27		
5		1372	2720	920	-7	
6		6416	18880	11604	1320	-46

Table 2.—continued

(d)  $k = 3$

$l \backslash j$	0	1	2	3
3	1			
4	40	20		
5	468	560	49	
6	3656	7168	2344	-44

(e)  $k = 4$

$l \backslash j$	0	1	2
4	0		
5	32	16	
6	640	768	$63\frac{1}{2}$

(f)  $k = 5$

$l \backslash j$	0	1
5	$-\frac{1}{3}$	
6	$13\frac{1}{3}$	$6\frac{2}{3}$

(g)  $k = 6$

$l \backslash j$	0
6	$-\frac{1}{6}$

Table 3. The coefficients  $A_{jkl}$  in the reduced susceptibility series for  $n = 3$ , simple cubic lattice.

$$\chi \approx \sum_{l=0}^5 \sum_{j+k \leq l} A_{jkl} (\beta J_{xy})^{l-j-k} R^j S^k.$$

(a)  $k = 0$  (all entries check with Lambeth and Stanley 1975).

$l \backslash j$	0	1	2	3	4	5
0	1					
1	4	2				
2	12	16	2			
3	$33\frac{6}{10}$	80	32	$\frac{8}{10}$		
4	$85\frac{6}{10}$	$326\frac{4}{10}$	240	$38\frac{4}{10}$	$-\frac{4}{10}$	
5	$206\frac{6}{5}$	1168	$1366\frac{4}{10}$	$457\frac{6}{10}$	$25\frac{6}{10}$	$-\frac{4}{7}$

Table 3.—continued

(b)  $k = 1$ 

$l \backslash j$	0	1	2	3	4
1	2				
2	16	8			
3	80	96	10		
4	$326\frac{4}{10}$	672	240	0	
5	1168	$3622\frac{4}{10}$	2360	$300\frac{8}{10}$	$-9\frac{76}{100}$

(c)  $k = 2$ 

$l \backslash j$	0	1	2	3
2	2			
3	32	16		
4	240	288	$26\frac{4}{10}$	
5	$1366\frac{4}{10}$	2720	$915\frac{2}{10}$	$-17\frac{92}{100}$

(d)  $k = 3$ 

$l \backslash j$	0	1	2
3	80		
4	$38\frac{4}{10}$	$19\frac{2}{10}$	
5	$457\frac{6}{10}$	$550\frac{4}{10}$	$45\frac{6}{10}$

(e)  $k = 4$ 

$l \backslash j$	0	1
4	$-\frac{4}{10}$	
5	$25\frac{6}{10}$	$12\frac{8}{10}$

(f)  $k = 5$ 

$l \backslash j$	0
5	$-\frac{4}{7}$

also Citteur and Kasteleyn 1972, 1973), which relate derivatives of  $\chi$  with respect to  $R$  to the two-dimensional susceptibility.

Specifically, Liu and Stanley showed that for  $S = 0$ ,

$$\partial\chi/\partial R|_{R=S=0} = 2J_{xy}(\chi_{sq})^2 = 2J_{xy} [\chi(R = 0, S = 0)]^2 \tag{5a}$$

where  $\chi_{sq}$  is the susceptibility of the two-dimensional square lattice. This result follows from noting that the graphs which contribute to the term in the susceptibility that is linear in  $R$ , consist of one  $R$  bond joining two arbitrary planar graphs in adjacent  $xy$  planes (cf figure 2(a)). Since these planar graphs lie in different  $xy$  planes, they are completely independent. Two inequivalent such configurations exist. Taking the derivative  $\partial\chi/\partial R$  and then setting  $R = 0$ , singles out only these contributions that are linear in  $R$ , and (5a) follows. A second check comes from applying the *same* argument to the  $R = 0$  case, with the result

$$\partial\chi/\partial S|_{R=S=0} = 2J_{xy}(\chi_{sq})^2 = 2J_{xy} [\chi(R = 0, S = 0)]^2. \tag{5b}$$

A third check involves the coefficient of  $\chi$  that is proportional to  $RS$ . The graphical contribution to this term consists of one  $R$  bond and one  $S$  bond, the endpoints of which connect to three planar graphs (cf figure 2(b)). Because  $R$  and  $S$  are of unequal length, these three planar graphs must be mutually independent. Eight inequivalent such configurations exist. These configurations are singled out by taking the derivative  $\partial^2\chi/\partial R\partial S$  and then setting  $R = S = 0$ . Thus we obtain

$$\partial^2\chi/\partial R\partial S|_{R=S=0} = 8J_{xy}^2(\chi_{sq})^3 = 8J_{xy}^2 [\chi(R = 0, S = 0)]^3. \tag{5c}$$

These theorems also hold if instead of using the variables  $R$  and  $S$ , the respective Ising variables

$$\rho \equiv \tanh(\beta J_z)/\tanh(\beta J_{xy}) \quad \text{and} \quad \sigma \equiv \tanh(\beta J'_z)/\tanh(\beta J_{xy})$$

are used. Thus to any order  $L$ , these checks verified  $2(L + 1)$  coefficients out of a total of  $(L + 1)(L + 2)/2$ .

Note that the  $n = 1$  susceptibility series of equation (2) (table 1) has the novel feature that the coefficients  $A_{437}$  and  $A_{448}$  are negative. This can be understood by the following graph-theoretic considerations. In general,  $A_{jkl}$  consists of the number of self-avoiding walks (SAW) that can be embedded on a lattice, with  $l-j-k$  bonds in the  $xy$  plane,  $j$  bonds in the  $z$  direction, and  $k$  bonds of length two in the  $z$  direction minus a disconnected graph

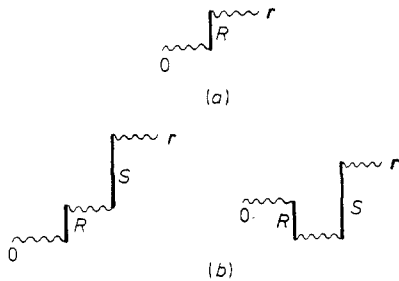


**Figure 2.** (a) The high-temperature graphs which contribute to the term proportional to  $R$  in the susceptibility. The wavy lines represent the set of all arbitrary bond configurations on one  $xy$  plane only. Another independent configuration is obtained by permuting 0 and  $r$ . (b) The graphs which contribute to the  $RS$  term in the susceptibility. Six more independent configurations are obtained by permuting the  $R$  and  $S$  bonds, and 0 and  $r$ .

contribution. This contribution is the number of disconnected graphs with the same number of bonds as the SAW, embedded so that bonds from disjoint graph pieces share the same lattice bond. In systems previously studied the SAW contribution predominates, and series coefficients are positive. However, the  $R$ - $S$  model possesses a much more complicated graph topology and affords the possibility of a large disconnected graph contribution due to multiple occurrences of disconnected graphs containing one  $S$  bond and two  $R$  bonds.

### 3. Scaling theory

Our analysis of critical properties in the ferromagnetic phase is guided by the generalisation of the scaling hypothesis to this system: there exist four numbers  $a_H$ ,  $a_\tau$ ,  $a_R$ , and  $a_S$  such that for all positive  $\lambda$ , (Hankey and Stanley 1972),

$$G(\lambda^{a_H}H, \lambda^{a_\tau}\tau, \lambda^{a_R}R, \lambda^{a_S}S) = \lambda G(H, \tau, R, S), \quad (6)$$

where  $G$  is the Gibbs potential,  $H$  is the magnetic field, and  $\tau(R, S) \equiv k[T(R, S) - T_c(0, 0)]/J_{xy}$ . The new scaling power  $a_S$  equals  $a_R$  since  $G(H, \tau, 0, S) = G(H, \tau, S, 0)$  (if  $R = 0$  and  $S \neq 0$ , the  $R$ - $S$  model reduces to two interpenetrating meta-models). A consequence of equation (6) is that  $\tau_c$  obeys the functional relationship

$$\tau_c(\lambda^{a_R}R, \lambda^{a_S}S) = \lambda^{a_\tau}\tau_c(R, S). \quad (7)$$

Setting  $\lambda^{a_R}R = 1$ , we obtain  $\tau_c(R, S) = R^{a_\tau/a_R}\tau_c(1, S/R)$ , while if  $\lambda^{a_S}S = 1$ , we have  $\tau_c(R, S) = S^{a_\tau/a_S}\tau_c(R/S, 1)$ . Thus along any ray in the ferromagnetic region of figure 1(b),  $\tau_c(R, S)$  varies as  $R^{1/\phi}$  and as  $S^{1/\phi}$  (where  $1/\phi = a_\tau/a_R = a_\tau/a_S$ ) with an amplitude that depends on the ray chosen. For the case  $n = 1$ , we test the validity of this prediction by using Padé analysis on the series to find  $\tau_c(R, S)$ . On a log-log plot of  $\tau_c$  versus  $R$ , a line of slope  $1/\phi = 4/7$  fits the small- $R$  data well, over a substantial range (cf figure 3). The breakdown of linearity is due to the fact that at very small  $R$ , the series are too short to find the critical temperature accurately, while for sufficiently large  $R$ , scaling is no longer valid

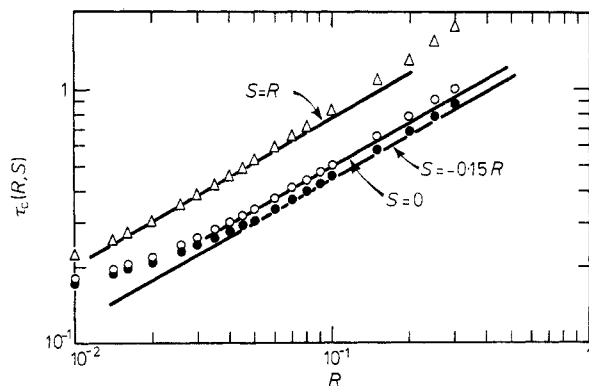


**Figure 3.** Log-log plot of  $\tau_c(R, S)$  versus  $R$  to test the scaling relation,  $\tau_c(R, S) = R^{a_\tau/a_R}\tau_c(1, S/R)$ . The inverse crossover exponent,  $\phi^{-1} = a_\tau/a_R$  is  $4/7$  (Abe 1970, Suzuki 1971, Liu and Stanley 1972, 1973). The straight lines have slope  $4/7$ . Data are shown for three representative rays in the ferromagnetic region of figure 1(b).

(Harbus and Stanley 1973a). For  $n = 2$  and 3 the series are too short to show a linear range when plotting  $\tau_c(R)$  versus  $R$  and thus data are not shown.

#### 4. The susceptibility exponents for the Ising and spherical models

When  $S < 0$  and  $R > 0$ , the interactions  $R$  and  $S$  compete. This competition is necessary for the appearance of helical order (cf figure 1(b)), and it is interesting to study the effect of this competition on the susceptibility as  $R$  and  $S$  vary. In what follows we set  $R = 1$  to eliminate crossover effects between two- and three-dimensional ordering. The series are analysed by complementary use of both ratio and Padé methods. The ratios  $\rho_l \equiv a_l/a_{l-1}$  oscillate when plotted against  $1/l$  due to the 'antiferromagnetic singularity'  $-\beta_{AF}$  on the negative  $\beta$  axis, found by examining the Padé table for the logarithmic derivative series for  $\chi$ . We reduce these oscillations by using the transformation  $\beta \rightarrow \beta/(1 + \beta/\beta_{AF})$  in order to extrapolate the  $l \rightarrow \infty$  behaviour of the  $\rho_l$ . Such a bilinear transformation introduces a new but spurious singularity at  $\beta_{SP}$  on the positive real axis (cf figure 4) which has a

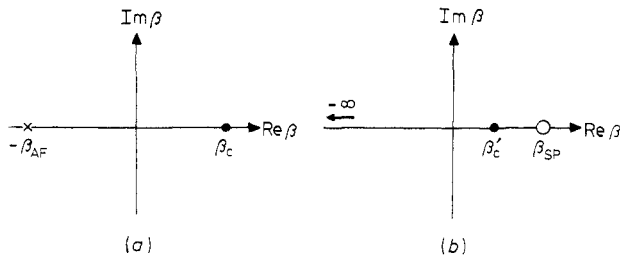


**Figure 4.** Singularity structure of the susceptibility series in the complex  $\beta$  plane, (a) before transformation, (b) after the bilinear transformation. The antiferromagnetic singularity is moved to  $-\infty$ , while a spurious singularity is introduced at  $+\beta_{AF}$ , and the physical singularity is moved to  $\beta'_c = \beta_c/(1 + \beta_c/\beta_{AF})$ . The second transformation we use removes the spurious singularity.

substantial effect on series extrapolations. The exponent associated with  $\beta_{SP}$  is equal to the negative of the susceptibility exponent (Paul and Stanley 1972). The effect of this new singularity on series extrapolations is minimised by multiplying the transformed series by  $(1 - \beta/\beta_{SP})^{\tilde{\gamma}}$ , where  $\tilde{\gamma}$  is a rough estimate for the susceptibility exponent. The series obtained after both transformations possesses a physical singularity which is isolated from all other singularities, and the ratios  $\rho_l$  vary smoothly in  $l$ . From the  $\rho_l$  we form the sequence of estimates  $\gamma_l \equiv 1 - l(1 - \rho_l/kT_l)$  for the susceptibility exponent  $\gamma$ , where  $kT_l \equiv l\rho_l - (l-1)\rho_{l-1}$  is a sequence of estimates for the critical temperature. The  $\gamma_l$  are shown in figure 5 for three representative values of  $S$ , based on Ising series. For  $n = 2$  and 3, the same trends in the  $\gamma_l$  are found as in the case  $n = 1$ . However, the  $n = 2$  and 3 series are too short to provide accurate estimates for  $\gamma$ , even when  $S = 0$ . Therefore, these data are not shown.

At first sight, the  $n = 1$  data indicate that  $\gamma$  does indeed depend on  $S$ . However comparison with a similar analysis of the corresponding  $n = \infty$  series (cf Appendix 2) shows that this is not the case. As shown in figure 6, for negative  $S$ , the  $\gamma_l$  eventually have a downward trend to the universal value of  $\gamma = 2$  (Joyce 1966). The trend appears for large  $l$ , and indicates that the critical region shrinks considerably as the Lifshitz point is

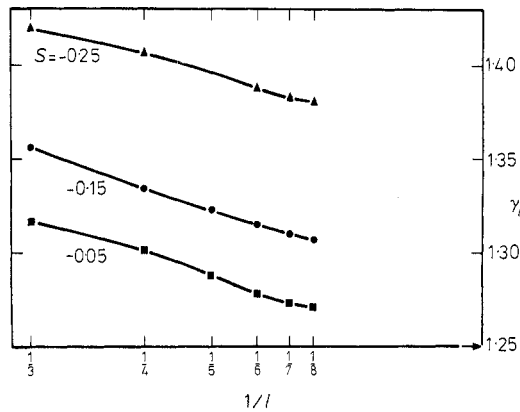


**Figure 5.** Plots of the successive estimates  $\gamma_i$ , for the susceptibility exponent based on Ising series for three representative values of  $S$ . The arrow marks the true value of  $\gamma$ .

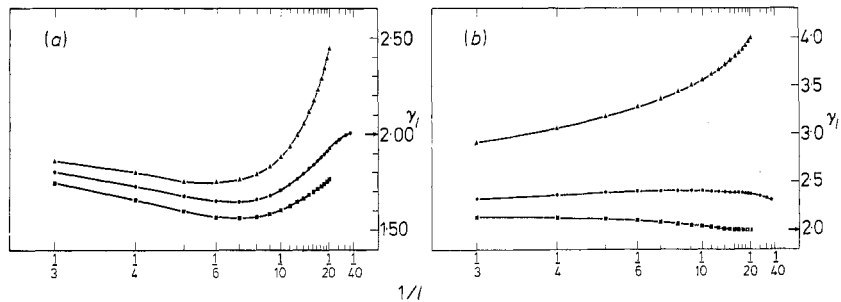


**Figure 6.** Plots of the successive estimates  $\gamma_i$ , for the susceptibility exponent based on the corresponding three-dimensional spherical model series. In (a) we show the results when the series are analysed by the methods described in the text. However, a Padé analysis of the raw series reveals an additional singularity on the positive real  $\beta$  axis located at  $\beta_{\text{add}}$ , with exponent  $-\lambda_{\text{add}}$ . This singularity is somewhat more distant from the origin than the physical singularity, and thus the convergence rate of series extrapolations to the physical singularity is reduced. Therefore for an improved analysis, we first multiply the raw series by  $(1 - \beta/\beta_{\text{add}})^{-\lambda_{\text{add}}}$  and then use the methods of the text. The resultant  $\gamma_i$  are shown in (b). Note that a downward trend in the  $\gamma_i$  occurs for  $l > 20$  when  $S = -0.15$ , and this trend is much more apparent in (b) than in (a).  $S = -0.25$  ( $\blacktriangle$ ),  $-0.15$  ( $\bullet$ ),  $-0.05$  ( $\blacksquare$ ).

approached. This can be understood physically by considering figure 7. When  $S = 0$  the system is isotropic (since  $R = 1$  here) and a 'correlated region' of spins is roughly speaking a sphere of diameter  $\sim \xi$ , where  $\xi$  is the correlation length. For a fixed value of  $T - T_c$ , as  $S$  decreases, the competition of  $R$  and  $S$  results in a corresponding decrease in the  $z$  correlation length, and the correlated region becomes more oblate. The number of enclosed spins thus decreases, and this reduces the degree of cooperativity in the system. Therefore, for negative  $S$ , one must probe closer to  $T_c$  by generating more series terms, in order that the asymptotic three-dimensional behaviour is evident. At the Lifshitz point, the  $z$  correlation length varies as the square root of the  $xy$  correlation length (Hornreich *et al* 1975a). This marks the point at which the effects of the competition between  $R$  and  $S$  are most pronounced. The shape of the correlated region is now *quantitatively* different, in

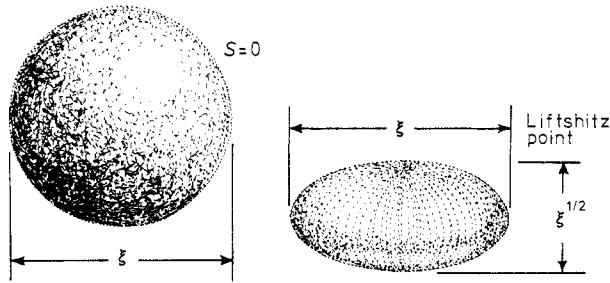


**Figure 7.** A correlated region of spins is a sphere of diameter  $\zeta$  for  $S = 0$ . For fixed  $T - T_c$ , as  $S$  decreases, and the correlated region becomes oblate. At the Lifshitz point  $\zeta_z \sim (\zeta_{xy})^{\frac{1}{2}}$ , giving rise to quantitatively different critical behaviour.

that the volume varies as  $\zeta^{d-\frac{1}{2}}$ , where  $d$  is the spatial dimension, rather than  $\zeta^d$ . From this argument it follows that the critical exponents are also different at the Lifshitz point.

We can gain more insight by looking at the  $n = \infty$  series in higher dimensions. Now ferromagnetic interactions exist in  $(d - 1)$ -dimensional layers, while competing interactions exist along one axis only. Therefore, the influence of these competing interactions should become relatively less important as  $d$  increases. This is reflected in our analysis, where for comparison with figure 6, we show in figure 8 the sequences  $\gamma_l$  for

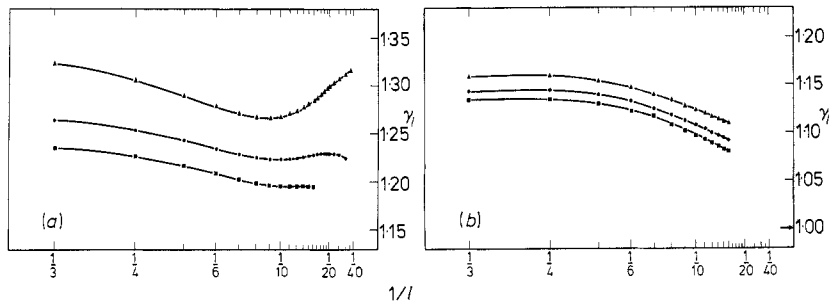


**Figure 8.** Dependence on  $1/l$  of  $\gamma_l$  for (a)  $d = 4$ , and (b)  $d = 5$  hypercubic lattices.  $S = -0.25$  ( $\blacktriangle$ ),  $-0.15$  ( $\bullet$ ),  $-0.05$  ( $\blacksquare$ ). The complications that occurred in analysing the three-dimensional series (cf figure 6) do not occur for  $d = 4, 5$ .

various  $S$  in both four and five dimensions. Furthermore, in five dimensions, it is clear that even when  $S = -\frac{1}{4}$ ,  $\gamma = 1$ , while in four dimensions it appears that  $\gamma \neq 1$  when  $S = -\frac{1}{4}$ . This indicates that the dimension at which mean field exponents first occur, the marginal dimensionality  $d_c$ , lies between four and five. In fact, from the Ginzburg criterion (Als-Nielsen and Birgeneau 1977 and references therein) it may be shown that  $d_c = 4.5$  (Hornreich *et al* 1975a). At dimension  $4.5$ , the volume of a correlated region grows as  $\zeta^{4.5-0.5} = \zeta^4$ , and thus mean-field exponents are expected.

5. The structure factor

In the previous section, we discussed how competing interactions influence the size of a correlated region. By translating the discussion into Fourier space language, we will obtain insight into the full dependence of the structure factor  $\mathcal{S}(\mathbf{q}) \equiv \sum_r \langle s_0 s_r \rangle \exp(i\mathbf{q} \cdot \mathbf{r})$  on both temperature and  $\mathbf{q}$ . In addition, we will see in a simple fashion why series extrapolations give misleading results at low order when  $R$  and  $S$  compete.

First consider  $S = 0$ . In figure 9(a) we sketch the dependence of  $\mathcal{S}(\mathbf{q}, T)$  on  $q_z$  and  $T$ . Since  $\chi(T) = \mathcal{S}(\mathbf{q} = 0, T)$ , the  $\mathbf{q} = 0$  structure factor diverges as  $T \rightarrow T_c$ , and this is reflected in extrapolations based on finite-length series for  $\chi$ . Now suppose  $q_z = \tilde{q}, q_x = q_y = 0$  where  $\tilde{q}$  is small. For this value of  $\mathbf{q}$ , the first few terms in a series for  $\mathcal{S}(\mathbf{q}, T)$  differ by only a small amount from the first few terms for  $\chi$ . Therefore as  $T$  decreases the structure factor  $\mathcal{S}(\mathbf{q}, T)$  initially increases and appears to extrapolate to infinity. However at  $T_c, \mathcal{S}(\mathbf{q}, T_c) \sim \tilde{q}^{-2+\eta}$ , which is finite, and in fact the structure factor appears to extrapolate to a divergence at some temperature below  $T_c$ . The extrapolations of  $\mathcal{S}(q_z, T)$  for a range of small  $q_z$  thus lead to a line of apparent singularities in the  $Tq_z$

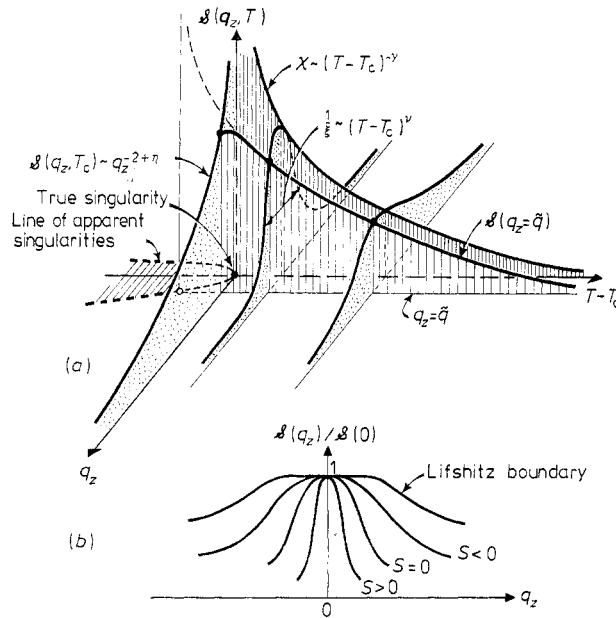


**Figure 9.** (a) The structure factor in  $Tq_z$  space, where  $\mathbf{q} = (q_x, q_y, q_z)$ . For  $\mathbf{q} = 0$  the structure factor is just the susceptibility, which diverges as  $T \rightarrow T_c$ . For fixed  $T$ , the width of the structure-factor peak is related to the inverse correlation length  $\xi^{-1}(T)$  which vanishes at  $T_c$  (for  $T = T_c$ , the structure factor varies as  $q_z^{-2+\eta}$ ). For  $q_z = \tilde{q}$ , where  $\tilde{q}$  is small, the limiting value of  $\mathcal{S}(\tilde{q}, T = T_c)$  is therefore finite; however extrapolations of finite-length structure-factor series will lead to an apparent singularity. Thus, in addition to the true singularity at  $q_z = 0$ , there will be an entire line of apparent singularities (broken line) in the  $Tq_z$  plane. (Note that the small maximum in  $\mathcal{S}(\tilde{q}, T)$  at positive  $T - T_c$  is expected from the work of Fisher and Burford 1967.)

(b) The dependence of the normalised structure factor on  $q_z$  for fixed  $T > T_c$ . For negative  $S$ , the correlation length is decreased and the peak broadens. At the Lifshitz point, the peak has a flatter top corresponding to the physical fact that fluctuations of many wavelengths are equally important.

plane (cf figure 9(a)). This line of apparent singularities interferes with extrapolations of  $\mathcal{S}(q = 0, T)$  to the physical singularity, just as nearby singularities in the complex  $\beta$  plane interfere with the physical singularity. As more terms in the structure factor series are computed, the range of  $q_z$  for which an extrapolated singularity appears becomes smaller. The physical singularity becomes more dominant, and extrapolations for  $\gamma$  improve.

Now consider  $S < 0$ . The interactions  $R$  and  $S$  now compete and the correlation length  $\xi$  is thus decreased relative to the case  $S = 0$ . Since  $\xi_z^{-1}$  is proportional to the halfwidth of  $\mathcal{S}(q_z, T)$ , the  $q_z \neq 0$  fluctuations in the structure factor are enhanced compared to  $q_z = 0$  fluctuations (cf figure 9(b)). This enhancement in fluctuations increases the range of  $q_z$  values for which an apparent singularity exists in  $\mathcal{S}(q_z, T)$ . Thus, it is necessary to compute correspondingly longer series in order that extrapolation techniques will converge to the physical singularity; this argument is verified by calculating the high-temperature series for the structure factor for the  $R$ - $S$  model.

It is interesting to note that the effect that we have described is a precursor of the transition to helical order; in the helical phase  $\mathcal{S}(q, T)$  diverges for some nonzero value of  $q$ . The onset of helical order is characterised by a structure factor independent of  $q_z^2$  to lowest order (cf figure 9(b)). When this occurs, the competition between the interactions  $R$  and  $S$  is maximised and series extrapolation methods converge quite slowly.

## 6. Conclusion

In summary, we have studied the  $R$ - $S$  model in which competing interactions strongly influence the properties of the ferromagnetic phase. We have calculated the high-temperature series to order 8, 6, 5, and 35 respectively for the Ising, planar, Heisenberg, and spherical models. These series were analysed for a range of  $R$  and  $S$  corresponding to the ferromagnetic phase; in particular for the Ising series we verified two-parameter scaling in both  $R$  and  $S$ . Near the Lifshitz point, we found by studying spherical model series, that asymptotic series behaviour is not evident unless quite lengthy series are analysed. This arises because of the competition between the interactions  $R$  and  $S$ . Geometrically, these ideas are simply understood by considering the full wavevector and temperature dependence of the structure factor  $\mathcal{S}(q, T)$ .

## Acknowledgment

The authors wish to thank Drs J F Nicoll, T S Chang, G F Tuthill, W Klein, A Hankey and especially Mr P J Reynolds for valuable discussions. The authors also thank Prof M Wortis who provided us with his  $R = 1, S = 0$  computer program.

## Appendix 1. Mean-field theory

The mean-field theory, while not generally providing correct predictions for critical behaviour, does give physical insight into many of the physical features of the  $R$ - $S$  model. In fact, series expansions may be regarded as a systematic improvement on the predictions of mean-field theory (e.g., the mean-field theory agrees with series expansions to lowest order).

One principal advantage of the mean-field theory is that it may be systematically

applied to yield unambiguous predictions for all four phases that occur for the  $R$ - $S$  model (cf. figure 1(b))†. To find the ordered phases, we minimise the classical energy. This is accomplished first by noting that the anisotropy in the system is along the  $z$  axis, and therefore below  $T_c$ , spatial variation in the spin expectation value occurs along the  $z$  axis. That is,  $s_r = \langle s_0 \rangle \cos \mathbf{q} \cdot \mathbf{r} = \langle s_0 \rangle \cos qz$  where  $s_0$  and  $s_r$  refer to the spin at the origin and at  $\mathbf{r}$  respectively, and  $\mathbf{q} = qz$  is the wavevector describing the ordered phase. The energy per spin becomes

$$E = -J_{xy}(4 + 2|R| \cos q + 2S \cos 2q) \langle s_0^2 \rangle = -\hat{J}(q) \langle s_0 \rangle^2 \quad (\text{A1.1})$$

where  $\hat{J}(q)$  is the Fourier transform of the exchange interactions in equation (1). Minimising equation (A1.1) with respect to  $q$  yields three solutions corresponding to commensurate order when  $S > -|R|/4$ , either ferromagnetic ( $q_0 = 0$ ) or antiferromagnetic ( $q_0 = \pi$ ), and incommensurate order,  $q_0 = \cos^{-1}(-|R|/4S)$  when  $S < -|R|/4$ .

The critical temperature at any point in the  $RS$  plane is found from the condition

$$kT_c = \hat{J}(q_0). \quad (\text{A1.2})$$

This may be written as  $kT_c = J_{xy}(4 + 2|R| + 2S)$  for commensurate order, and

$$kT_c = J_{xy}(4 + 2|R| \cos q_0 + 2S \cos 2q_0) = J_{xy}(4 - R^2/4S - 2S)$$

for incommensurate order, and from these formulae, we can describe the critical surface. For the commensurate phases, the lines of constant  $T_c$  are inclined at an angle of  $45^\circ$  with respect to the  $R$  or  $S$  axes, and these lines form part of the diamond-shaped figure shown in figure A1.1(a). Therefore, the critical surface consists of two planar sections, each of which is inclined from the horizontal  $RS$  plane by an angle of  $\tan^{-1}\sqrt{8}$ .

In the incommensurate phases, the critical surface can be illustrated by considering the critical line for fixed  $R$ , and decreasing  $S$ , starting from the Lifshitz boundary. This curve initially drops, and then there is a broad trough at  $S = -|R|/\sqrt{8}$  (cf figure A1.1(b)). As  $S \rightarrow -\infty$ , the curve becomes asymptotically linear, and  $kT_c \cong J_{xy}(4 - 2S)$ . Therefore, the critical surface becomes a plane inclined from the horizontal  $RS$  plane by an angle of  $\tan^{-1}2$ . These geometric features are shown in figure A1.1.

Finally, the nature of the phase transition can be studied as  $T \rightarrow T_c^+$  by considering the structure factor,

$$\begin{aligned} \mathcal{S}(q) &= [kT - \hat{J}(q)]^{-1} \\ &= \{kT - J_{xy}[4 + 2|R| + 2S - q^2(|R| + 4S) + \frac{1}{12}q^4(|R| + 16S) \\ &\quad \dots]\}^{-1} \\ &= \left\{ t + q^2 \left( \frac{|R| + 4S}{4 + 2|R| + 2S} \right) - \frac{1}{12}q^4 \left( \frac{|R| + 16S}{4 + 2|R| + 2S} \right) + \dots \right\}^{-1}. \end{aligned} \quad (\text{A1.3})$$

Here  $t \equiv [T - T_c(0)]/T_c(0)$ , and  $T_c(0)$  is the critical temperature at  $q = 0$ . When  $S > -|R|/4$  the coefficient of  $q^2$  in (A1.3) is positive, and a minimum of  $\mathcal{S}^{-1}(q)$  occurs at  $q = 0$  (cf figure A1.2). This corresponds to the fact that at any  $T > T_c$ , the largest fluctuations are for  $q = 0$ , and as  $T \rightarrow T_c^+$  these fluctuations (the susceptibility) diverge, while fluctuations for  $q \neq 0$  remain finite.

However, when  $S < -|R|/4$ , the coefficient of  $q^2$  in (A1.3) is now negative and a minimum of  $\mathcal{S}^{-1}(q)$  occurs at nonzero  $q$ . An approximate expression for  $q^2$  may be found

† Many results of mean-field theory are well known, and useful pedagogical accounts may be found in Brout (1965) and Smart (1966).

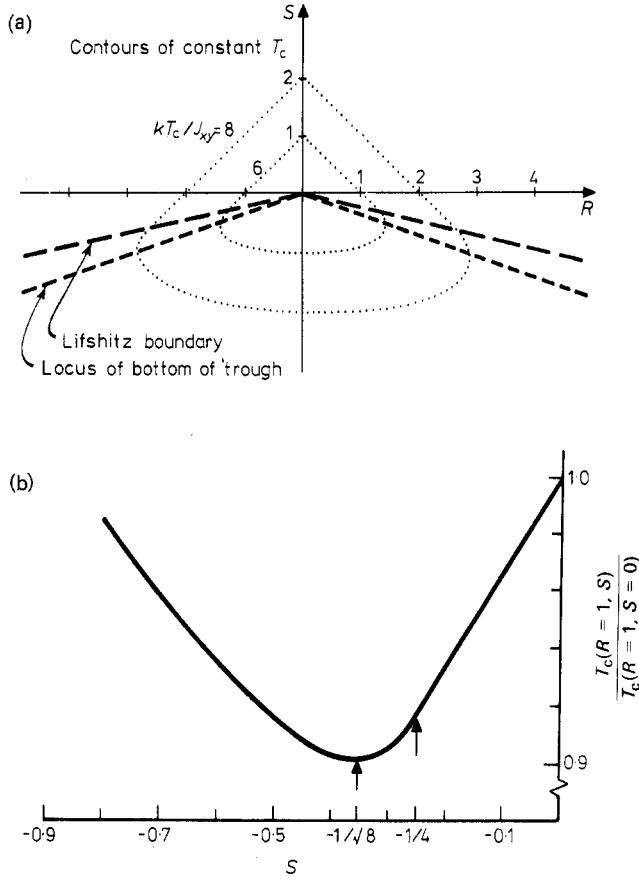


**Figure A1.1.** (a) A map of the critical surface in the  $RS$  plane, showing contours of constant  $T_c$ . A broad trough in this surface occurs at  $S = -|R|/\sqrt{8}$ . (b) A critical line for  $R = 1$ , and varying  $S$ . Note the exaggerated vertical scale so that the trough is readily apparent.

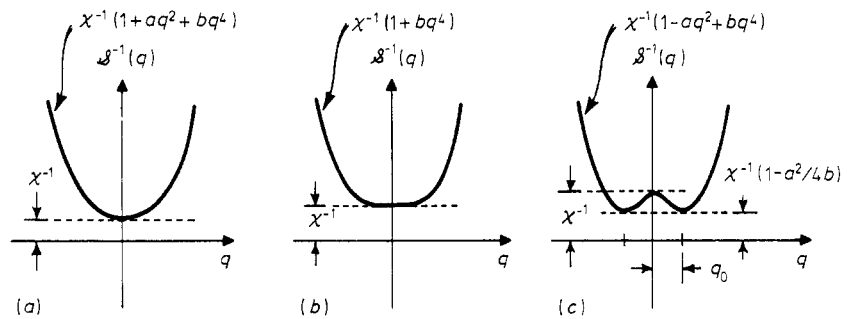


**Figure A1.2.** The inverse structure factor for fixed  $T > T_c$ , in the ferromagnetic and helical phases, and at the Lifshitz point. The minimum of  $\mathcal{S}(q)^{-1}$  determines the ordered phase wavevector  $q_0$ , and this may be found by minimising  $\mathcal{S}(q)^{-1}$ . (a) Uniform order,  $S > -|R|/4$ ; (b) Lifshitz point,  $S = -|R|/4$ ; (c) helical order,  $S < -|R|/4$ .

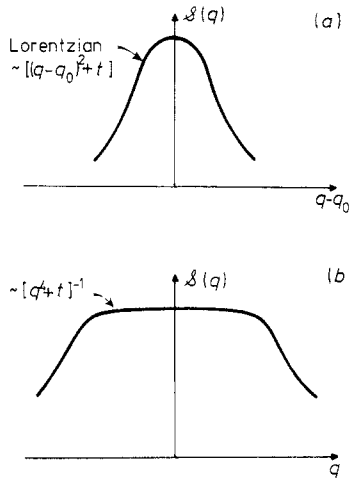


**Figure A1.3.** The  $q$  dependence of the structure factor for fixed  $t \equiv (T - T_c)/T_c > 0$ . (a)  $S > -|R|/4$ ,  $q_0 = 0$  or  $S < -|R|/4$ ,  $q_0 \neq 0$ ; (b)  $S = -|R|/4$ ,  $q_0 = 0$ . At the Lifshitz point the coefficient of  $q^2$  in (A1.3) vanishes, and the peak is not a Lorentzian. However, in both the ferromagnetic and helical phases the peak is a Lorentzian centred about  $q_0$ .

by minimising  $\mathcal{S}^{-1}(q)$  with respect to  $q$ ,

$$q_0^2 \cong -6(|R| + 4S)/(|R| + 16S). \tag{A1.4}$$

This expression agrees with  $q_0 = \cos^{-1}(-|R|/4S)$  to lowest order in  $1 + |R|/4S$ . As  $T \rightarrow T_c^+$ ,  $\mathcal{S}(q_0)$  diverges, and fluctuations for all  $q \neq q_0$  remain finite (cf figure A1.2). The onset of helical order occurs when  $|R| + 4S = 0$ , and here the coefficient of  $q^2$  in (A1.3) vanishes. This condition marks the transition point between the dominance of nonzero wavelength and zero wavelength fluctuations, and therefore the transition can be regarded as an ‘instability in Fourier space’. At this instability, fluctuations of small nonzero wavevector are just as important as zero wavelength fluctuations for  $T > T_c$ , and the structure factor is no longer Lorentzian, but rather is much less peaked about  $q = 0$  (cf figure A1.3). Hence, one might expect that the critical behaviour of a system at such an instability is markedly different than the usual critical behaviour, and this is found to be the case (Hornreich *et al* 1975a).

Physically, the condition  $|R| + 4S = 0$  also marks the point at which the competing influences of the  $R$  and  $S$  interactions just balance. When this occurs, spin correlations in the  $z$  direction are drastically reduced (cf figure 7) and the nature of the phase transition is quantitatively changed.

**Appendix 2. The spherical model**

We consider the  $R$ - $S$  Hamiltonian in the spherical model limit for arbitrary dimensionality  $d$ ,

$$\mathcal{H} = -J_{d-1} \left( \sum_{i,j}^{d-1} S_i S_j + R \sum_{i,j}^z S_i S_j + S \sum_{i,j}^{2z} S_i S_j \right) \tag{A2.1}$$

where the first sum is over nearest-neighbour spin pairs in the same  $(d - 1)$ -dimensional layer, while the last two sums are over nearest-neighbour and next-nearest-neighbour spin pairs along one axis (the  $z$  axis). The spins  $s_i$  can assume any finite value subject to the constraint  $\sum_i s_i^2 = N$  where  $N$  is the number of spins in the system. It will be more convenient to rewrite (A2.1) in the following form,

$$\mathcal{H} = -\frac{1}{2} \sum_{i,j} J_{ij} s_i s_j. \quad (\text{A2.2})$$

Most of the thermodynamic properties of this system are determined by the location of the partition function saddle-point, and this is given by the condition (Berlin and Kac 1952, Joyce 1966),

$$\sum_j J_{0j}/k_B T = \frac{1}{(2\pi)^d} \int d\omega \left( z_{\text{sp}} - \sum_j J_{0j} \cos \omega \cdot \mathbf{j} / \sum_j J_{0j} \right)^{-1} \quad (\text{A2.3})$$

where  $\mathbf{j}$  is the vector distance between the origin and site  $j$ ,  $z_{\text{sp}}$  is the saddle-point location, and the integral is over the first Brillouin zone. We define

$$J = \sum_j J_{0j} \quad \text{and} \quad f(\omega) \equiv \sum_j J_{0j} \cos \omega \cdot \mathbf{j} / \sum_j J_{0j}$$

and now equation (A2.3) can be written compactly as,

$$\begin{aligned} J/k_B T &= \frac{1}{(2\pi)^d} \int d\omega (1 - f(\omega)/z_{\text{sp}})^{-1} \\ &= \frac{1}{(2\pi)^d} \frac{1}{z_{\text{sp}}} \sum_{l=0}^{\infty} \int d\omega \left( \frac{f(\omega)}{z_{\text{sp}}} \right)^l \end{aligned} \quad (\text{A2.4})$$

$$\equiv \sum_{l=0}^{\infty} P_l / z_{\text{sp}}^{l+1}. \quad (\text{A2.5})$$

The last equality defines  $P_l$ , and for the  $R$ - $S$  model in  $d$  dimensions we have explicitly,

$$P_l = \frac{1}{(2\pi)^d} \int \left[ \frac{\cos \omega_1 + \cos \omega_2 + \cdots + \cos \omega_{d-1} + R \cos \omega_d + S \cos \omega_d}{(d-1) + R + S} \right]^l d\omega \quad (\text{A2.6})$$

and this integral may be evaluated directly.

The zero-field susceptibility can be expressed in terms of the saddle point as (Berlin and Kac 1952),

$$\chi = (k_B T/J)(z_{\text{sp}} - 1)^{-1}. \quad (\text{A2.7})$$

Thus to generate the high-temperature susceptibility series, we need to revert to the series in equation (A2.5) in order to express  $1/z_{\text{sp}}$  as a series in  $J/k_B T$ . That is, we have

$$z_{\text{sp}}^{-1} \equiv \sum_{l=0}^{\infty} Q_l (J/k_B T)^l. \quad (\text{A2.8})$$

Substitution of this series in equation (A2.7) then leads to the desired result.

**References**

- Abe R 1970 *Prog. Theor. Phys.* **44** 339–47
- Als-Nielsen J and Birgeneau R J 1977 *Am J. Phys.* **45** 554–60
- Berlin T H and Kac M 1952 *Phys. Rev.* **86** 821–35
- Brout R B 1965 *Phase Transitions* (Reading, Mass.: Benjamin)
- Citteur C A W and Kasteleyn P W 1972 *Phys. Lett. A* **42** 143–4
- 1973 *Physica* **68** 491–510
- Droz M and Coutinho-Filho M D 1976 *AIP Conf. Proc.* **29** 465–6
- Elliott R 1961 *Phys. Rev.* **124** 346–53
- Fisher M E and Burford R J 1967 *Phys. Rev.* **156** 583–622
- Garel A T 1976 *PhD thesis* Université de Paris-Sud
- Garel A T and Pfeuty P 1976 *J. Phys. C: Solid St. Phys.* L245–9
- Hankey A M A and Stanley H E 1972 *Phys. Rev.* **B6** 3515–42
- Harbus F I and Stanley H E 1973a *Phys. Rev. B* **8** 2268–72
- 1973b *Phys. Rev. B* **7** 365–70
- Hornreich R M, Luban M and Shtrikman S 1975a *Phys. Rev. Lett.* **35** 1678–81
- 1975b *Phys. Lett. A* **55** 269–70
- 1976 *Physica A* **86** 465–70
- Joyce G S 1966 *Phys. Rev.* **146** 349–57
- Lambeth D N and Stanley H E 1975 *Phys. Rev.* **B12** 5302–14
- Liu L L and Stanley H E 1972 *Phys. Rev. Lett.* **29** 927–31
- 1973 *Phys. Rev. B* **8** 2279–98
- Nicholl J F, Chang T S and Stanley H E 1976a *Phys. Rev.* **A13** 1251–64
- Nicholl J F, Tuthill G F, Chang T S and Stanley H E 1976b *Phys. Lett.* **A58** 1–2
- Oitmaa J and Enting I G 1971 *Phys. Lett. A* **36** 91–2
- 1972 *J. Phys. C: Solid St. Phys.* **5** 231–44
- Paul G and Stanley H E 1971 *Phys. Lett. A* **37** 347–9
- 1972 *Phys. Rev. B* **5** 2578–99
- Rapaport D 1971 *Phys. Lett.* **A37** 407–8
- Redner S and Stanley H E 1977 *Phys. Rev.* **B16**
- Smart J S 1966 *Effective Field Theories of Magnetism* (Philadelphia: Saunders)
- Suzuki M 1971 *Prog. Theor. Phys.* **46** 1054–70
- Wortis M, Jasnow D, and Moore M A 1969 *Phys. Rev.* **135** 805–15
- Wortis M 1974 in *Phase Transitions and Critical Phenomena* vol 3, eds C Domb and M S Green (London: Academic) 113–80